

Wireless Energy Transmission for Micro Aerial Vehicles Using a Microwave Phased Array

Ryoji Ozawa,* Hiroki Takayanagi,† Kimiya Komurasaki,‡ Yoshihiro Arakawa,§ Kenta Katsunaga,** and Hanno Ertel††

The University of Tokyo, Tokyo 113-8656, Japan

Wireless energy transmission for an Unmanned/Micro Aerial Vehicle (MAV) has been studied. Electric power for MAV's propulsion system is provided remotely from the ground power station using 5.8-GHz microwaves. A microwave beam is pointed to the MAV using the phased array technology. The minimum reception antenna radius and maximum steering angle are found in a trade-off relationship. With a two-dimensional array of five 110 mm × 81 mm antennas, 30% of radiated energy can be transmitted to the reception area of 180 mm radius at the height of 2 m.

I. Introduction

AT the university of Tokyo, a project for Unmanned Aerial Vehicle and Micro Aerial Vehicle, "Innovative Aerial Robot Project", is being carried out as part of the 21st century COE program, "Mechanical Systems Innovation". In this project, the transmission of microwave energy to MAV using a phased array antenna is considered.

The microwave phased array technology has been intensively developed for energy transmission in space,^[1,2] such as the transmission from a Space Solar Power Station to the ground. This technology is applied in this project: Pointing of the microwave beams is to be achieved by phase control of element microwaves rather than mechanical control of the antennas' attitude.

The basic concept is shown in Fig. 1. A MAV will fly in circles. It is planned to track the flying object using the retro-directive function.^[3,4]

This paper describes the current status of system development for the microwave phased array. The spatial power profile was measured and compared with the numerical simulation. In the final stage of the project, flight demonstration will be conducted.

II. Energy Transmission Using a Microwave Phased Array

Figure 2 shows the concept of beam direction control by a phased array. Theoretical relationship between the phase difference ϕ and steering angle θ is expressed as

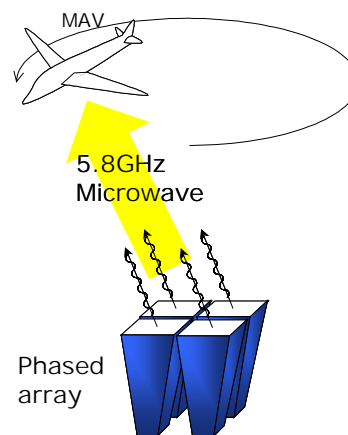


Figure 1. Schematic of microwave energy transmission to MAV.

* Graduate Student, Dept. Aero. & Astro., Hongo 7-3-1, Bunkyo, Tokyo 113-8656.

† Graduate Student, Dept. Aero. & Astro., Hongo 7-3-1, Bunkyo, Tokyo 113-8656.

‡ Associate Professor, Dept. Advanced Energy, Kashiwanoha 5-1-5, Kashiwa 277-8561, Senior Member.

§ Professor, Dept. Aero. & Astro., Hongo 7-3-1, Bunkyo, Tokyo 113-8656, Senior Member.

** Graduate Student, Dept. Advanced Energy, Kashiwanoha 5-1-5, Kashiwa 277-8561.

†† Graduate Student, Dept. Advanced Energy, Kashiwanoha 5-1-5, Kashiwa 277-8561.

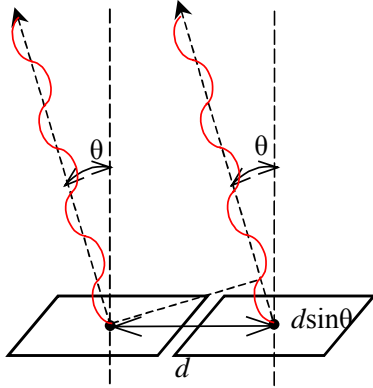


Figure 2. Beam Steering by phase control.

$$d \sin \theta = \lambda (\phi / 2\pi) \quad (1)$$

where, d is the array pitch and λ is the wavelength. Maximum steering angle θ_{\max} is obtained with $\phi = \pi$ as,

$$\theta_{\max} = \arcsin(\lambda / 2d) \quad (2)$$

It is well known that the profile usually consists of a central-lobe and multiple side-lobes. Side-lobe intensity is getting larger with the higher order oscillation modes. Since it is disadvantageous to collect the power in the side-lobes from the viewpoint of receiver size, especially for the transmission to mobile objects such as beam-powered vehicles, only the central-lobe is used for energy transmission.^[5]

In addition, to minimize the receiver area, a microwave oscillation frequency of 5.8 GHz was selected instead of 2.45 GHz, both of which are permitted for the purpose of scientific researches in open area. The corresponding wavelength λ is 5.17 cm.

III. Experimental Setup

Figure 3 shows the schematic of a 1×3 phased array transmitter system. 5.8 GHz microwave is provided by a Field Effect Transistor (FET) oscillator (ArumoTech Co.) and divided into three elements using a power divider. The phase of the element microwave is controlled individually using two 6-bit phase shifters, whose phase resolution is 5.6 deg. The phase shifters are controlled by a PC.

Three FET amplifiers with the output power of 1 watt each are used to have totally 3 watts output power. Each microwave is guided to an antenna through a coaxial cable and a waveguide. In this experiment, a horn antenna, whose exit plane size is $\Delta x = 110$ mm and $\Delta y = 81$ mm, is used as an element transmitter. (Fig. 4)

Three horn antennas are arranged in the x direction as shown in Fig. 5. As indicated in Eq. (2), θ_{\max} is almost inversely proportional to d . Currently, minimum array pitch between elements was limited to 110 mm by the size of horn antenna and corresponding θ_{\max} was 13.6 deg.

The power profile has been measured using a patch antenna set on a traverse stage. To minimize the microwave reflection on wall surfaces of the experimental room, the surfaces are covered by absorbers.

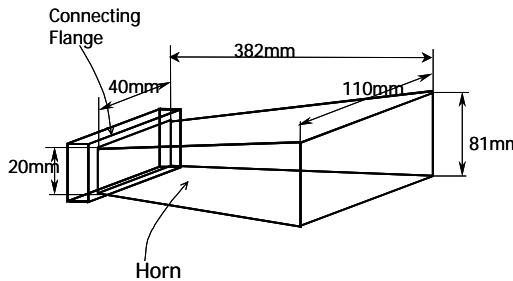


Figure 4. A horn antenna.

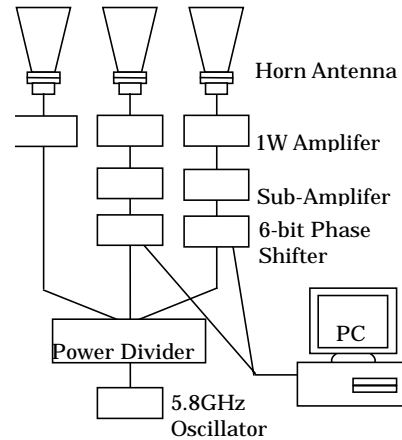


Figure 3. Microwave Phased Array System.

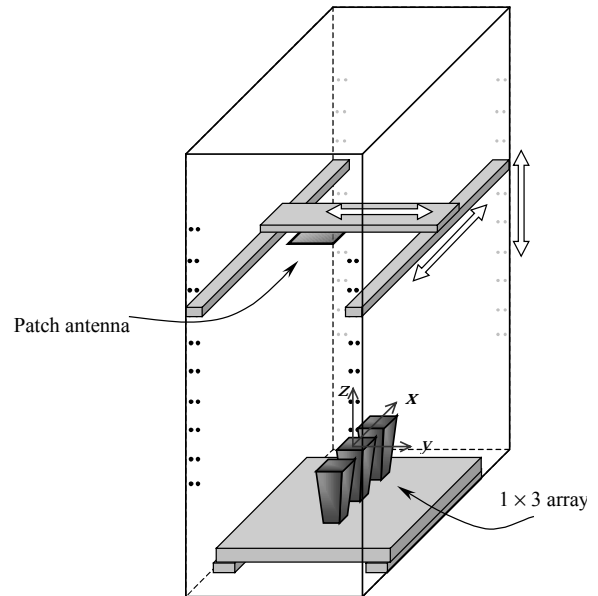


Figure 5. A 1×3 array system.

IV. Computational Model

In order to consider actual power profiles on each horn antenna and optimize geometric parameters of the array, electric field is numerically integrated and special profile of power was computed. Each element of an array was assumed as a diffraction-limited Gaussian beam. The electric-field distribution E at the transmitter surface $\mathbf{r}'(x', y', 0)$ is expressed as,

$$E_y(\mathbf{r}') = E_0 \sin\left[\frac{\pi(x' - x_i)}{\Delta x}\right], \quad (3)$$

where x_i and E_0 are the center position of i th element and electric-field amplitude at x_i , respectively. The electric-field distribution of a beam at the position $\mathbf{r}(x, y, h)$ is derived from the generalized Huygens-Fresnel integral acting on the input field;

$$E_i(\mathbf{r}) = \frac{1}{4\pi} \int_{y_i - \Delta y/2}^{y_i + \Delta y/2} \int_{x_i - \Delta x/2}^{x_i + \Delta x/2} E_i(\mathbf{r}') e^{-j\frac{2\pi}{\lambda}l} \frac{1}{l} \left[j\frac{2\pi}{\lambda} + \left(j\frac{2\pi}{\lambda} + \frac{1}{l} \right) \cos\theta \right] dx'dy', \quad l = |\mathbf{r} - \mathbf{r}'|, \quad \cos\theta = \hat{\mathbf{h}} \cdot (\mathbf{r} - \mathbf{r}')/l. \quad (4)$$

If all of the laser beams were coherent and in phase to form a completely coherent phased array, intensity of the resulting beam is expressed as

$$I(\mathbf{r}) = \left| \sum_i E_i(\mathbf{r}) \right|^2. \quad (5)$$

V. Beam Quality of the Central Lobe

A. Measured Beam Waist of the Central Lobe

Figure 6 showed a measured power profile using a patched antenna at the height $h=600$ mm. The beam waist of the central-lobe is estimated by fitting a Gaussian curve to the measured power profiles. Figure 7 shows the beam waist with a single horn antenna as well as with a 1×3 array. As shown in the figure, the beam waist was very large for a single horn, and it was drastically reduced for a 1×3 array despite the large antenna area. The waist difference in the x and y directions results from the size difference in the x and y directions of the horn.

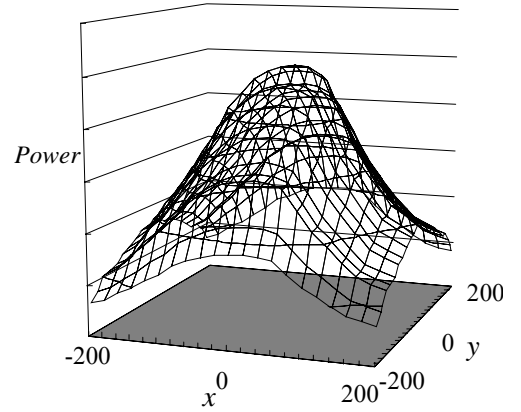


Fig. 6 Measured power profile for a single horn antenna at $h=600$ mm.

B. Numerical Prediction of the Beam Quality

Computed beam waist for the 1×3 array is plotted in Fig. 8 along with the measured one. It shows a good

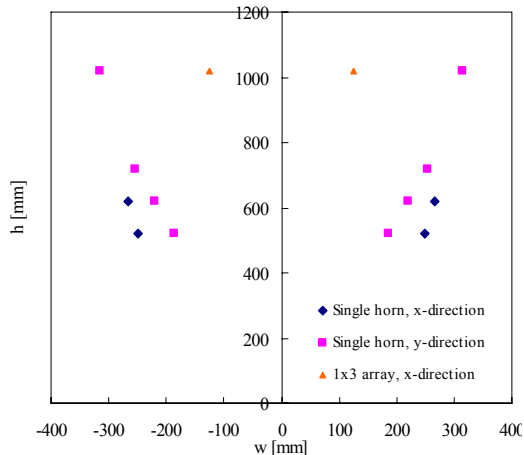


Figure 7. Measured beam waist for a single horn antenna and a 1×3 array.

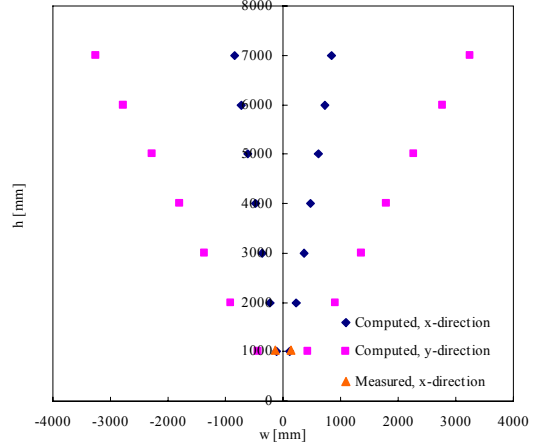


Figure 8. Computed beam waist for a 1×3 array.

agreement between computation and measurement. Therefore, this computation code can be used to evaluate the beam quality and to optimize the array design. Estimated beam divergence angle in the array direction (x -direction) θ_d is 7 deg. Since the beam divergence angle θ_{d0} of the diffraction limited beam with transmitter area equivalent to the array area can be estimated as

$$\tan\theta_{d0} = \lambda/\pi/(d+0.5\Delta x) = 5.7\text{deg}, \quad (6)$$

the beam quality factor of the central-lobe is

$$M^2 = \tan\theta_d / \tan\theta_{d0} = 1.23. \quad (7)$$

C. Steering Angle and Fractional Energy Contained in the Central-lobe

Figure 9 shows the effect of the beam steering angle θ on θ_d and the fractional energy η contained in the central-lobe. Although θ_d is almost constant, η is decreased with d and becomes 0.4 at $\theta = \theta_{\max}$. The energy has been dissipated in the side-lobes.

D. Array Pitch and Fractional Energy Contained in the Central-lobe

Figure 10 shows the effect of array pitch d on M^2 and η . M^2 is preserved with the increase in d , and then θ_d is inversely proportional to d . However, η is decreased with d because its transverse mode of the combined beam profile on the array surface becomes poor with the increase in $d/\Delta x$.^[5]

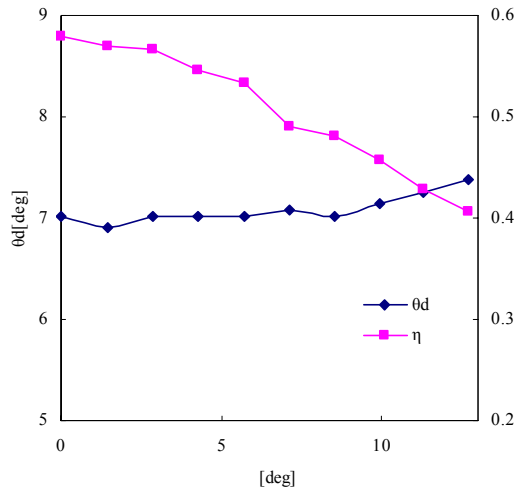


Figure 9. Beam divergence angle and fractional energy contained in the central-lobe for a 1×3 array. $d=110\text{mm}$.

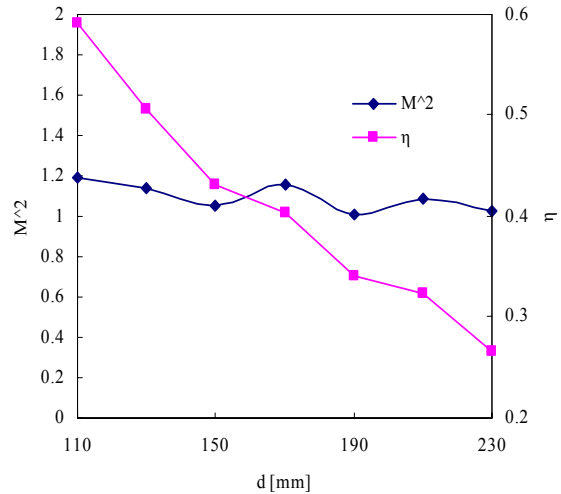


Figure 10. Beam quality factor and fractional energy contained in the central-lobe for a 1×3 array. $\theta=0$ deg.

VI. Two-Dimensional Beam Steering

A. Two-Dimensional Phased Array

Figure 11 shows a two-dimensional phased array with five element antennas. This would be an array of minimum number of elements.

Figure 12 shows the computed η as a function of θ for the two-dimensional array. η is slightly smaller for the steering in the x direction than in the y direction though θ_d is almost the same for both directions. Therefore, when a beam is pointed to a vehicle circling at a fixed angle, power fluctuation will be kept within $\pm 5\%$.

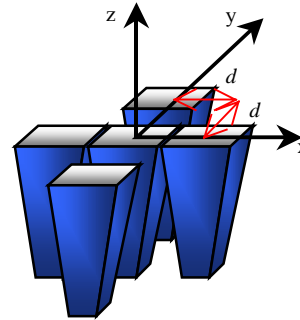


Figure 11. A two-dimensional phased array with five element antennas.

B. Required Reception Antenna Size

Transmittable power is a function of reception antenna area as well. Figure 13 shows the necessary reception antenna radius r at the height $h=2$ m for various d . Fractional transmission power is graphed as a parameter. Energy conversion losses at the transmitter and the receiver are not taken into account. As shown in the figure, if 30% energy transmission is expected, r takes a minimum value at $d/\Delta x = 1$. This is because η decreases with $d/\Delta x$ due to its poor transverse mode, and this effect dominates the opposite effect in which θ_d decreases with d due to large array area. (See Eq.(6)) For large fractional energy and large d cases, there is no plot because required energy exceeds the energy contained in the central-lobe. Minimum reception antenna radius is $r=180$ mm for 30 % energy transmission.

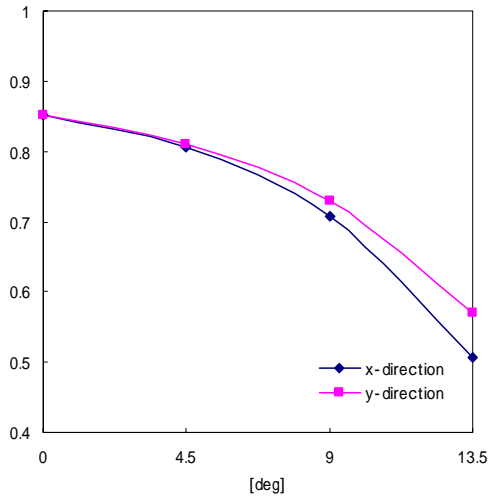


Figure 12. η v.s. steering angle.

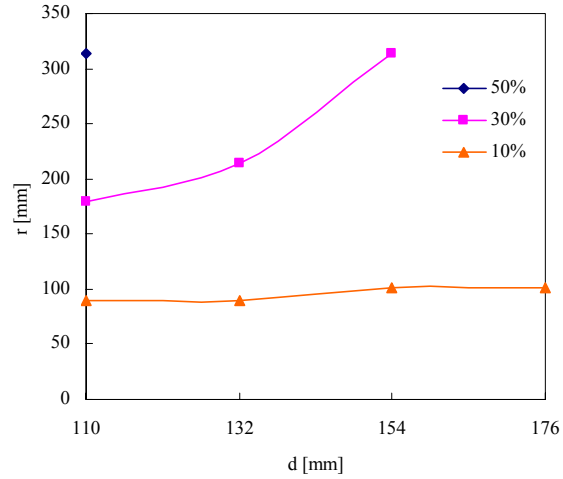


Figure 13. Array pitch and necessary reception antenna radius at $h=2000$ mm for a array of 110 mm \times 81 mm antennas

An array of five 55 mm \times 40 mm antennas with the same arrangement as shown in Fig. 11 is also considered. Figure 14 shows the computed η variation with θ . Large steering angle becomes available without a serious decrease in η . Figure 15 shows the necessary reception antenna radius for array of 55 mm \times 40 mm antennas. Similar tendency has been obtained with an array of 110 mm \times 81 mm antennas. Minimum r becomes twice due to the increase in θ_d .

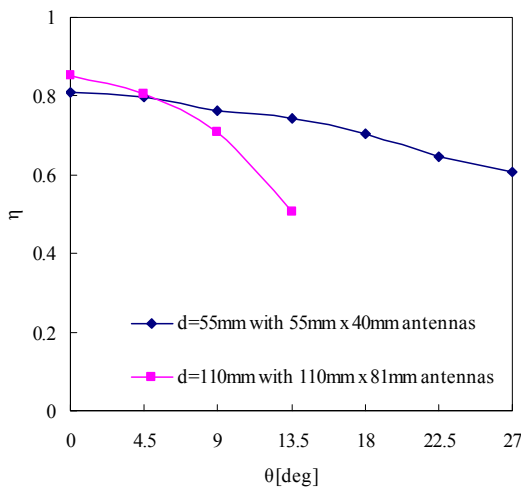


Figure 14. Fractional Energy and a steering angle for arrays of 55 mm \times 40 mm and 110 mm \times 81 mm antennas.

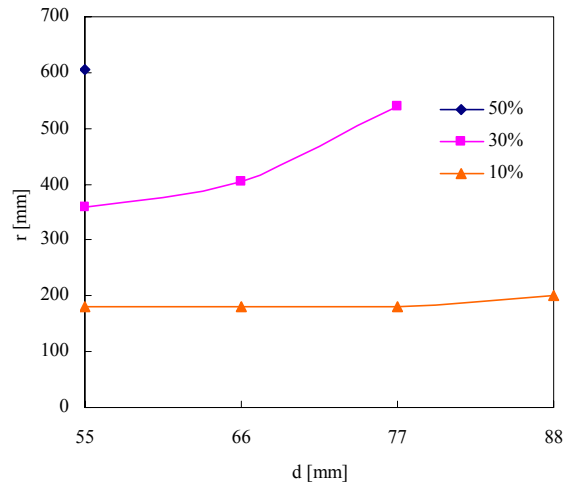


Figure 15. Array pitch and necessary reception radius for an array of 55 mm \times 55 mm antennas at $h=2000$ mm.

C. Proposed Array Geometry

Based on the above discussion, the minimum reception antenna radius and the maximum steering angle are found in a trade-off relationship for a limited number of array elements. If a MAV can circle at a very small circling radius or hover over the transmitter, a small steering angle is acceptable. Then, a large Δx gives a good beam convergence and a small reception antenna. As far as r is smaller than array size, the relationship can be expressed as

$$\frac{r}{h} = \frac{4.53}{\Delta x[\text{mm}]} \quad (8)$$

When r is comparable to or smaller than Δx , beam focusing would be effective to have a good beam convergence.

VII. Conclusion

Wireless energy transmission to an Unmanned/Micro Aerial Vehicle using the phased array technology has been studied. The computation code we developed successfully reproduced the measured beam quality of the antenna array.

Using this computation code, the effects of geometric parameters of the array, such as the array pitch, antenna size, and steering angle, were investigated. As a result, the minimum reception antenna radius and maximum steering angle are found in a trade-off relationship: With a two-dimensional array of five $110 \text{ mm} \times 81 \text{ mm}$ antennas, 30% of radiated energy can be transmitted to the reception area of 180 mm radius at the height of 2 m, though its steering angle is limited to 13.6 deg.

If a MAV can circle at a very small circling radius or hover over the transmitter, larger antennas than the ones tested can be selected to have a better beam convergence and a smaller reception antenna.

References

¹Shinohara N., Matsumoto H., "Experimental study of large rectenna array for microwave energy transmission," *IEEE Trans. on Microwave theory and Techniques*, Vol. 46, No. 3, 1998, pp. 261-268.

²Kaya N., Kojima H., Matsumoto H., et al., "ISY-METS Rocket Experiment for Microwave Energy Transmission," *Acta Astronautica*, Vol. 34, 1994, pp. 43-46.

³Yen S. C., and Chu T. H., "A retro-directive antenna array with phase conjugation circuit using sub-harmonically injection-locked self-oscillating mixers," *IEEE Trans. on Antennas and Propagation*, Vol. 52, No. 1, 2004, pp.154-164.

⁴Fusco V. F., Roy R., Karode S. L., "Reflector effects on the performance of a retrodirective antenna array," *IEEE Trans. on Antennas and Propagation*, Vol. 48, No. 6, 2000, pp. 946-953.

⁵Komurasaki, K., Nakagawa, T., Ohmura, S., Arakawa, Y., "Energy Transmission in Space Using an Optical Phased Array," *Trans. JSASS, Space Technology Japan*, Vol. 3 (2005), pp.7-11.

: